**RESEARCH**

**Open Access**

# Distinct mutations with different inheritance mode caused similar retinal dystrophies in one family: a demonstration of the importance of genetic annotations in complicated pedigrees

Xue Chen[1,2,3†], Xunlun Sheng[4†], Yani Liu[4†], Zili Li[4†], Xiantao Sun[5], Chao Jiang[1], Rui Qi[4], Shiqin Yuan[4], Xuhui Wang[4], Ge Zhou[4], Yanyan Zhen[4], Ping Xie[1], Qinghuai Liu[1], Biao Yan[2,3*] and Chen Zhao[1,2,3,5*]

## Abstract

**Background:** Retinitis pigmentosa (RP) is the most common form of inherited retinal dystrophy presenting remarkable genetic heterogeneity. Genetic annotations would help with better clinical assessments and benefit gene therapy, and therefore should be recommended for RP patients. This report reveals the disease causing mutations in two RP pedigrees with confusing inheritance patterns using whole exome sequencing (WES).

**Methods:** Twenty-five participants including eight patients from two families were recruited and received comprehensive ophthalmic evaluations. WES was applied for mutation identification. Bioinformatics annotations, intrafamilial co-segregation tests, and in silico analyses were subsequently conducted for mutation verification.

**Results:** All patients were clinically diagnosed with RP. The first family included two siblings born to parents with consanguineous marriage; however, no potential pathogenic variant was found shared by both patients. Further analysis revealed that the female patient carried a recurrent homozygous *C8ORF37* p.W185*, while the male patient had hemizygous *OFD1* p.T120A. The second family was found to segregate mutations in two genes, *TULP1* and *RP1*. Two patients born to consanguineous marriage carried homozygous *TULP1* p.R419W, while a recurrent heterozygous *RP1* p.L762Yfs*17 was found in another four patients presenting an autosomal dominant inheritance pattern. Crystal structural analysis further indicated that the substitution from arginine to tryptophan at the highly conserved residue 419 of TULP1 could lead to the elimination of two hydrogen bonds between residue 419 and residues V488 and S534. All four genes, including *C8ORF37*, *OFD1*, *TULP1* and *RP1*, have been previously implicated in RP etiology.

**Conclusions:** Our study demonstrates the coexistence of diverse inheritance modes and mutations affecting distinct disease causing genes in two RP families with consanguineous marriage. Our data provide novel insights into assessments of complicated pedigrees, reinforce the genetic complexity of RP, and highlight the need for extensive molecular evaluations in such challenging families with diverse inheritance modes and mutations.

**Keywords:** Retinitis pigmentosa, Genetic heterogeneity, Next generation sequencing, Mutation, *OFD1*, *C8ORF37*, *TULP1*, *RP1*, Consanguinity

*Correspondence: yanbiao1982@hotmail.com; dr_zhaochen@163.com
†Xue Chen, Xunlun Sheng, Yani Liu and Zili Li contributed equally to this work
[1] Department of Ophthalmology, State Key Laboratory of Reproductive Medicine, The First Affiliated Hospital of Nanjing Medical University, Nanjing, China
Full list of author information is available at the end of the article

Chen *et al. J Transl Med* (2018) 16:145

Page 2 of 12

## Background

Retinitis pigmentosa (RP, MIM: 268000), the most common form of inherited retinal degenerations, affects over one million individuals globally [1, 2]. Night blindness is usually the initial symptom for RP, followed by subsequent visual field constriction, and eventual vision loss. RP is featured by great clinical heterogeneities. Its onset age ranges from early childhood to mid-adulthood. Inter- and intra-familial phenotypic diversities caused by the same RP causing mutations have also been revealed [3–5]. Thus, clinical diagnose for RP patients are sometimes challenged by its wide phenotypic spectrum and under certain conditions, like in a young patient without fully onset RP phenotypes. In such situations, molecular testing could help to address the clinical ambiguity in RP diagnosis. RP also shows high genetic heterogeneity. To date, 83 RP causing genes involving hundreds of mutations have been identified (RetNet). Next-generation sequencing (NGS), enabling simultaneous parallel sequencing of numerous genes with high efficiency, is an efficient tool for molecular diagnosis of RP [2, 4]. Genetic annotations with NGS promote better clinical assessments and gene therapy, and therefore should be recommended for RP patients. However, pedigrees with puzzling inheritance patterns could sometimes confuse the genetic diagnoses. Herein, we described the genotypic and phenotypic findings in two complicated RP pedigrees using NGS. Distinct inheritance patterns and RP causing genes/mutations were found in both families.

## Methods

### Sample collection and clinical assessments

Our study, conformed to the Declaration of Helsinki, was approved and prospectively reviewed by the local ethics committee of People Hospital of Ningxia Hui Autonomous Region (No. 10 [2017]). Eleven participants from family A (Fig. 1a) and 14 participants from family B (Fig. 1b) were recruited from the People's Hospital of Ningxia Hui Autonomous Region. Written informed contents were obtained from all participants or their legal guardians before their enrollments. Peripheral blood samples were collected from all 25 participants

for genomic DNA extraction. Family history and consanguineous marriages were carefully reviewed. Medical records were obtained from all participants. Each participant received general ophthalmic evaluations, while comprehensive ophthalmic examinations were selectively conducted on the eight included patients. Another 150 Chinese healthy controls free of major ocular problems were recruited with their blood samples donated.
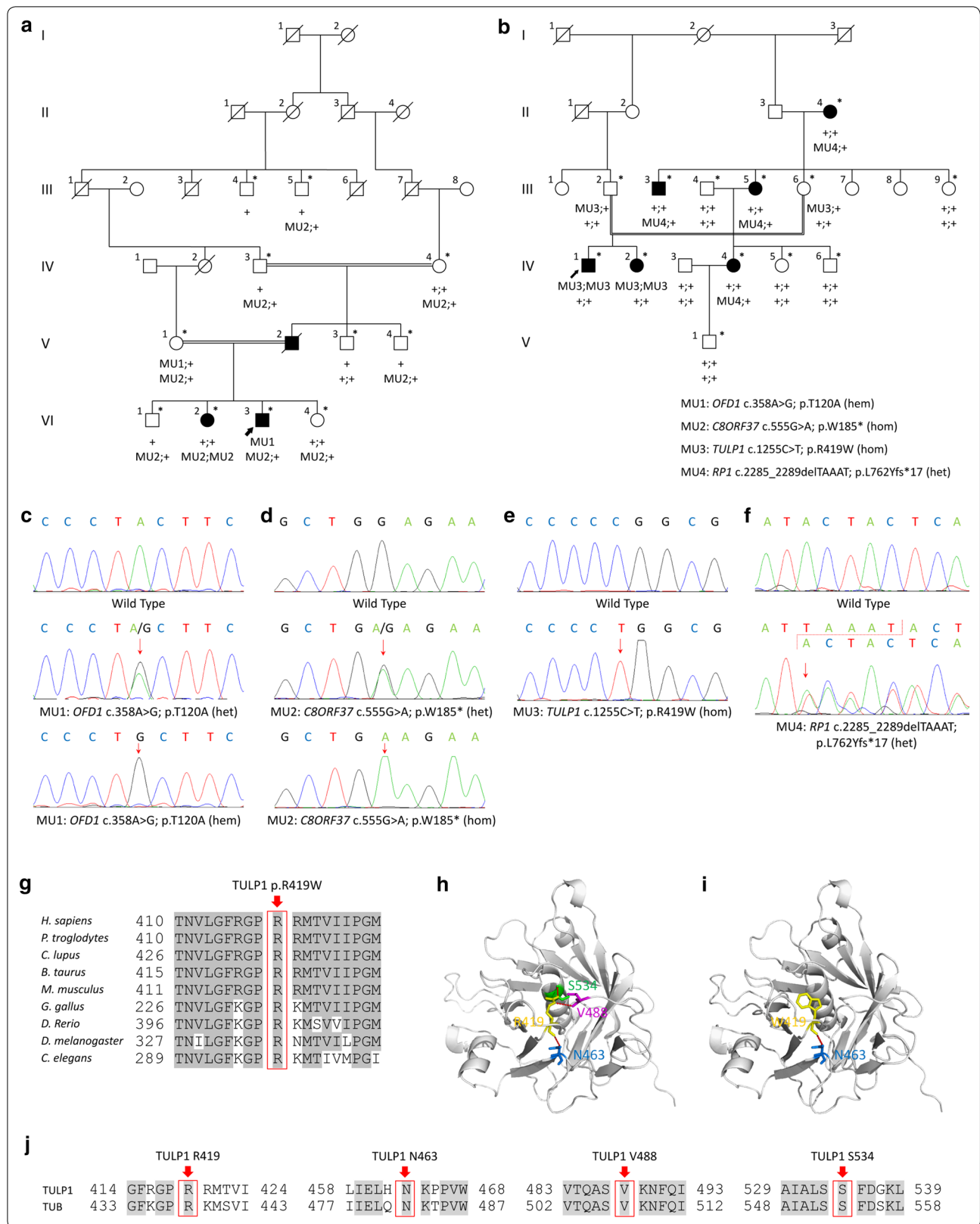
### NGS approach and bioinformatics analyses

To reveal the disease causing mutation in the two families, we selectively performed whole exome sequencing (WES) on three participants in family A (A-IV:3, A-VI:2 and A-VI:3) and two patients in family B (B-III:4 and B-IV:1). WES was conducted with the 44.1 megabases SeqCap EZ Human Exome Library v2.0 (Roche NimbleGen, Madison, WI) for enrichment of 23588 genes on patients from family A [6], and with SureSelect Human All Exon V6 60 Mb Kit (Agilent Technologies, Santa Clara, CA) on patients from family B [7]. Briefly, qualified genomic DNA samples were randomly sheared by Covaris into 200–250 base pair (bp) fragments. Fragments were then ligated with adapters to both ends, amplified by ligation-mediated polymerase chain reaction (LM-PCR), purified, and hybridized. Non-hybridized fragments were then washed out. Quantitative PCR was further applied to estimate the magnitude of enrichment of both non-captured and captured LM-PCR products. Each post-capture library was then loaded on an Illumina Hiseq 2000 platform for high-throughput sequencing.

Raw data were initially processed by CASAVA Software 1.7 (Illumina) for image analysis and base calling. Sequences were generated as 90 bp pair-end reads. Reads were aligned to human h19 genome using SOAPaligner (http://www.soap.genomics.org.cn) and Burrows-Wheeler Aligner (BWA; http://www.bio-bwa.sourceforge.net/). Only mapped reads were included for subsequent analysis. Coverage and depth were determined based on all mapped reads and the exome region. Atlas-SNP2 and Atlas-Indel2 were applied for variant calling [8]. Variant frequency data were obtained from the following six single nucleotide polymorphism databases, including

(See figure on next page.)
**Fig. 1** Family pedigrees and genetic annotations of identified mutations. **a** Pedigree of family A. Included participants are indicated by asterisk. **b** Pedigree of family B. Included participants are indicated by asterisk. **c–f** Sequence chromatograms of identified mutations, including *OFD1* c.358A>G (**c**), *C8ORF37* c.555G>A (**d**), *TULP1* c.1255C>T (**e**), and *RP1* c.2285_2289delTAAAT (**f**). **g** Orthologous protein sequence alignment of TULP1 from human (*H. sapiens*), chimpanzees (*P. troglodytes*), dogs (*C. lupus*), cows (*B. taurus*), rats (*M. musculus*), chickens (*G. gallus*), zebrafish (*D. rerio*), fruit flies (*D. melanogaster*), and worms (*C. elegans*). Conserved residues are shaded. The mutated residue 419 is boxed and indicated. **h, i** Crystal structural analysis of the wild type (**h**) and mutant (**i**) TULP1 protein. Hydrogen bonds between residue 419 and residues V488 and S534 were eliminated due to the substitution from arginine to tryptophan. **j** Conservational analysis of residues TULP1 R419, N463, V488 and S534 between TULP1 and TUB proteins

Chen *et al. J Transl Med* (2018) 16:145

Page 3 of 12



a

b

MU1: *OFD1* c.358A>G; p.T120A (hem)

MU2: *C8ORF37* c.555G>A; p.W185* (hom)

MU3: *TULP1* c.1255C>T; p.R419W (hom)

MU4: *RP1* c.2285_2289delTAAAT; p.L762Yfs*17 (het)

c

C C C T A C T T C

Wild Type

C C C T A/G C T T C

MU1: *OFD1* c.358A>G; p.T120A (het)

C C C T G C T T C

MU1: *OFD1* c.358A>G; p.T120A (hem)

d

G C T G G A G A A

Wild Type

G C T G A/G A G A A

MU2: *C8ORF37* c.555G>A; p.W185* (het)

G C T G A A G A A

MU2: *C8ORF37* c.555G>A; p.W185* (hom)

e

C C C C C G G C G

Wild Type

C C C C T G G C G

MU3: *TULP1* c.1255C>T; p.R419W (hom)

f

A T A C T A C T C A

Wild Type

A T T A A A T A C T
A C T A C T C A

MU4: *RP1* c.2285_2289delTAAAT;
p.L762Yfs*17 (het)

g

TULP1 p.R419W

| | | | |
|---|---|---|---|
| *H. sapiens* | 410 | TNVLGFRGP | R | RMTVIIPGM |
| *P. troglodytes* | 410 | TNVLGFRGP | R | RMTVIIPGM |
| *C. lupus* | 426 | TNVLGFRGP | R | RMTVIIPGM |
| *B. taurus* | 415 | TNVLGFRGP | R | RMTVIIPGM |
| *M. musculus* | 411 | TNVLGFRGP | R | RMTVIIPGM |
| *G. gallus* | 226 | TNVLGFKGP | R | KMTVIIPGM |
| *D. Rerio* | 396 | TNVLGFKGP | R | KMSVVIPGM |
| *D. melanogaster* | 327 | TNILGFKGP | R | NMTVILPGM |
| *C. elegans* | 289 | TNVLGFKGP | R | KMTIVMPGI |

h

S534
V488
R419
N463

i

R419
N463

j

TULP1 R419     TULP1 N463     TULP1 V488     TULP1 S534

| | | | | | | | | | | | |
|---|---|---|---|---|---|---|---|---|---|---|---|
| TULP1 | 414 | GFRGP | R | RMTVI | 424 | 458 | LIELH | N | KPPVW | 468 | 483 VTQAS V KNFQI 493 | 529 AIALS S FDGKL 539 |
| TUB | 433 | GFKGP | R | KMSVI | 443 | 477 | IIELQ | N | KTPVW | 487 | 502 VTQAS V KNFQI 512 | 548 AIALS S FDSKL 558 |

Chen *et al. J Transl Med* (2018) 16:145

Page 4 of 12

**Table 1 Clinical features of attainable patients**

| Family member ID | RP causative gene | Age (year)/sex | Onset age (year) | Night blindness | Cataract | | BCVA (logMAR) | | Fundus appearance | | | | | | | | ERG | |
|---|---|---|---|---|---|---|---|---|---|---|---|---|---|---|---|---|---|---|
| | | | | | | | | | O.D. | | | | O.S. | | | | | |
| | | | | | O.D. | O.S. | O.D. | O.S. | MD | OD | AA | PD | MD | OD | AA | PD | O.D. | O.S. |
| A-V:2[a] | – | – | 10 | Yes | – | – | LP | LP | – | – | – | – | – | – | – | – | – | – |
| A-VI:2 | C8ORF37 | 25/F | 8 | Yes | No | No | LP | LP | Yes | Waxy | Yes | Yes | Yes | Waxy | Yes | Yes | D | D |
| A-VI:3 | OFD1 | 24/M | 2 | Yes | No | No | LP | LP | Yes | Waxy | Yes | Yes | Yes | Waxy | Yes | Yes | D | D |
| B-II:4 | RP1 | 80/F | 50 | Yes | Severe | Severe | NLP | LP | – | – | – | – | Yes | Waxy | Yes | Yes | – | D |
| B-III:3 | RP1 | 59/M | 30 | Yes | IOL | IOL | 0.6 | 0.25 | Yes | Waxy | Yes | Yes | Yes | Waxy | Yes | Yes | D | D |
| B-III:5 | RP1 | 54/F | 35 | Yes | Mild | Mild | 0.3 | 0.3 | Yes | Waxy | Yes | Yes | Yes | Waxy | Yes | Yes | D | D |
| B-IV:1 | TULP1 | 27/M | EC | Yes | Moderate | Moderate | 0.15 | 0.2 | Yes | Waxy | Yes | Yes | Yes | Waxy | Yes | Yes | D | D |
| B-IV:2 | TULP1 | 24/F | EC | Yes | Moderate | Moderate | 0.3 | 0.3 | Yes | Waxy | Yes | Yes | Yes | Waxy | Yes | Yes | D | D |
| B-IV:4 | RP1 | 31/F | – | Yes | No | No | 0.5 | 0.8 | No | No | No | Yes | No | No | No | Yes | R | R |

*F* female, *M* male, *EC* early childhood, *BCVA* best corrected visual acuity, *logMAR* logarithm of the minimum angle of resolution, *O.D.* right eye, *O.S.* left eye, *IOL* intraocular lens, *LP* light perception, *NLP* non-light perception, *MD* macular degeneration, *OD* optic disk, *AA* artery attenuation, *PD* pigment deposits, *ERG* electroretinography, *D* diminished, *R* reduced

[a] This patient is deceased. His clinical features are obtained based on his medical records

Chen *et al. J Transl Med* (2018) 16:145

Page 5 of 12

dbSNP144 (http://www.hgdownload.cse.ucsc.edu/golde nPath/hg19/database/snp135.txt.gz.), HapMap Project (ftp://ftp.ncbi.nlm.nih.gov/hapmap), 1000 Genome Project (ftp://ftp.1000genomes.ebi.ac.uk/vol1/ftp), YH database (http://yh.genomics.org.cn/), Exome Variant Server (http://www.evs.gs.washington.edu/EVS/), and Exome Aggregation Consortium (http://exac.broad institute.org/). Variants with a minor allele frequency of over 1% in any of the above databases were discarded. Sanger sequencing was employed for mutation validation and prevalence test in 150 additional controls using a previously defined protocol [9]. Primer information is detailed in Additional file 1: Table S1 and Additional file 2: Table S2.

### In silico analysis

We applied vector NTI Advance™ 2011 software (Invitrogen, Carlsbad, CA) to analyze the conservation of the mutated reside by aligning protein sequence of human TULP1 (ENSP00000229771) with sequences of the following orthologues proteins: *P. troglodytes* (ENSP-TRP00000030898), *C. lupus* (ENSCAFP00000001922), *B. taurus* (ENSBTAP00000055698), *M. musculus* (ENS-MUSP00000049070), *G. gallus* (ENSGALP00000010281), *D. rerio* (ENSDARP00000099556), *D. melanogaster* (FBpp0088961), and *C. elegans* (F10B5.4). Crystal structural modeling of the wild type and mutant TULP1 proteins were constructed with SWISS-MODEL online server [10, 11], and displayed with PyMol software.

## Results

### Clinical findings

Two patients from family A, A-VI:2 and A-VI:3, and six patients from family B, B-II:4, B-III:3, B-III:5, B-IV:1, B-IV:2 and B-IV:4, were included in the present study with their clinical details summarized in Table 1. Ophthalmic features of patient A-V:2 were obtained according to his medical records, and were presented in Table 1. All patients from the two families were clinically diagnosed with RP. In family A, all three patients had early onset nyctalopia and rapid disease progress. Best corrected visual acuity was light perception for both patients A-VI:2 and A-VI:3 at their last visit to our hospital at the ages of 25 and 24 respectively. Typical RP presentations and macular degeneration were detected upon their ophthalmic evaluations (Fig. 2A–G and Table 1). In family B, RP onset ages ranged from early childhood to 50 years old (Table 1). RP progression also varied among the 6 patients. Patients B-IV:1 and B-IV:2 reported to have nyctalopia since early childhood, while the other four patients showed RP symptoms elder than 30-year-old. On examination, typical RP presentations were detected for all 6 patients, while patient B-II:4 also had chronic

angle closure glaucoma in her right eye (Fig. 2H–S). Noteworthy, all 6 patients presented mild to severe cataracts (Table 1). Patient B-III:3 received bilateral cataract surgeries 2 years ago. No systemic defect was noticed in any of the included patients.

### Genetic assessments

To identify the pathogenic mutations, WES with high quality was selectively performed on individuals A-IV:3, A-VI:2, and A-VI:3 from family A (mean coverage: 98.16%; mean depth: 70.89×), and patients B-III:5 and B-IV:1 from family B (mean coverage: 98.32%; mean depth: 104.66×). NGS data were summarized in Additional file 3: Table S3. Exon-specific coverage report of all known RP genes was presented in Additional file 4: Table S4. For family A, patients A-VI:2 and A-VI:3 were born to parents with consanguineous marriage, supporting potential autosomal recessive inheritance. WES identified 10 homozygous variants and 6 compound heterozygous variants shared by patients A-VI:2 and A-VI:3 (Additional file 1: Table S1). However, Sanger sequencing revealed no variant co-segregated with the disease phenotype. We thus hypothesized that the two patients may have distinct RP causing mutations. Based on WES data, patient A-VI:2 carried a recurrent homozygous *C8ORF37* mutation c.555G>A (p.W185*; Fig. 1d and Table 2), while patient A-VI:3 had a novel hemizygous *OFD1* mutation c.358A>G (p.T120A; Fig. 1c and Table 2).

As to family B, WES revealed one homozygous variant and 18 compound heterozygous variants shared by patients B-III:4 and IV:2 (Additional file 2: Table S2), while no variant was validated co-segregated with the disease phenotype. According to the family pedigree, patients B-IV:1 and B-IV:2 were born to unaffected parents with consanguineous marriage, indicating a potential autosomal recessive inheritance pattern. However, the RP phenotypes of patients B-III:3 and B-III:4 were likely inherited from the affected mother B-II:4, suggesting a dominant inheritance mode. Upon this hypothesis, a novel homozygous *TULP1* mutation c.1255C>T (p.R419W; Fig. 1e and Table 2) was revealed as RP causative for patients B-IV:1 and B-IV:2, and a recurrent heterozygous *RP1* mutation c.2285_2289delTAAAT (p.L762Yfs*17; Fig. 1f; Table 2) was found in patients B-II:4, B-III:3 and B-III:4. The mutated residue R419 in TULP1 was highly conserved among all tested species (Fig. 1g). Crystal structures of the wild type and mutant TULP1 proteins were obtained based on human TUB protein (Protein Data Bank ID: 1S31) with a sequence identify of 75.19 and a sequence similarity of 0.54. Our data suggested that the substitution from arginine to tryptophan at residue 419 would lead to the elimination of two hydrogen bonds between residue 419 and residues

Chen *et al. J Transl Med* (2018) 16:145

Page 6 of 12
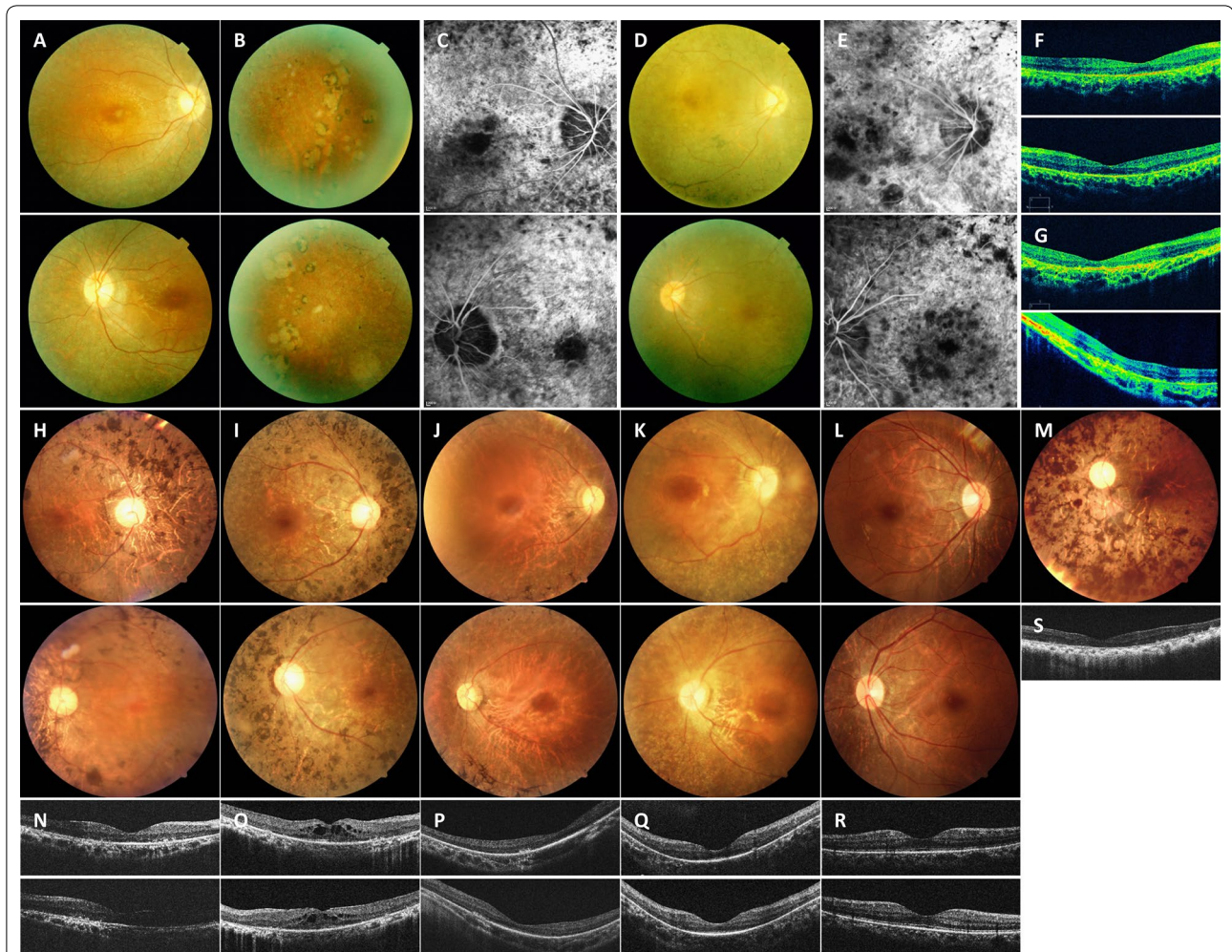


**Fig. 2** Ophthalmic presentations of included patients. **A**, **B** Fundus presentations of patient A-VI:3 (age 24, carrying *OFD1* c.358A>G) indicate waxy optic disc, attenuated retinal arterioles, macular degeneration, bone spicule-like pigments and atrophy of RPE and choroid in the peripheral retina. **C** Fundus fluorescein angiography (FFA) of patient A-VI:3 notices a combination of speckled hypofluorescent and hyperfluorescent changes in both macular and peripheral retina. **D** Fundus photos of patient A-VI:2 (age 27, carrying *C8ORF37* c.555G>A) show similar presentations to patient A-VI:3, but with more intensive pigmentations. **E** FFA of patient A-VI:2 also demonstrates intensive speckled changes of both hypofluorescence and hyperfluorescence. **F** OCT results of patient A-VI:3 indicate attenuated outer nuclear layer (ONL) and RPE with remarkable loss of inner segments (IS) and outer segments (OS). **G** OCT results of patient A-VI:2 show complete loss of IS and OS. **H** Patient B-III:3 (age 59, carrying *RP1* c.2285_2289delTAAAT) has a waxy optic disc, attenuated retinal arterioles, mild macular degeneration, and intensive bone spicule-like pigment deposits in the mid-peripheral retina of both eyes. **I** Patient B-III:5 (age 54, carrying *RP1* c.2285_2289delTAAAT) shows typical RP fundus similar to patient B-III:3, including intensive pigmentations and macular degeneration. **J** Fundus of patient B-IV:1 (age 27, carrying *TULP1* c.1255C>T) demonstrates attenuated retinal vessels, a waxy optic disc, remarkable macular degeneration, and diffuse pigment deposits in the periphery retina of both eyes. **K** Patient B-IV:2 (age 24, carrying *TULP1* c.1255C>T) shows similar fundus presentation to patient B-IV:1, presenting maculopathy and diffused pigmentations. **L** Slight waxy pallor of the optic disc and diffuse pigment deposits in the peripheral retina are revealed in the fundus of patient IV:4 (age 31, carrying *RP1* c.2285_2289delTAAAT). **M** Patient II:4 (age 80, carrying *RP1* c.2285_2289delTAAAT) shows typical RP fundus with intensive pigment deposits. **N** OCT results of patient B-III:3 indicate attenuated ONL and RPE with loss of IS and OS. **O** Thickened ONL with cystic cavities in the macular region were noticed by OCT in patient B-III:5. **P** OCT examinations of patient B-IV:1 demonstrate attenuated ONL and RPE with complete loss of IS and OS. **Q** Patient B-IV:2 shows similar OCT results to patient B-IV:1, including attenuated ONL and RPE, and loss of IS/OS. **R** Slightly attenuated ONL is presented in patient B-IV:4. **S** Typical RP presentations are revealed in patient B-II:4, demonstrating attenuated ONL and RPE with loss of IS and OS

V488 and S534 (Fig. 1h, i), further supporting that this mutation would disturb the tertiary structure of TULP1 and interrupt its function. Residues R419, N463, V488 and S534 were conserved between TULP1 and TUB proteins (Fig. 1j). All four mutations identified in the two families segregated with the disease phenotype (Fig. 1a,

Chen *et al. J Transl Med* (2018) 16:145

Page 7 of 12

**Table 2 Mutations identified in this study**

| Gene | Variation | | Status | Bioinformatics analysis | | | Reported or Novel | Population prevalence (allele count) | | |
|------|-----------|--|--------|-------------------------|--|--|-------------------|--------------------------------------|--|--|
| | Nucleotide | Amino acid | | SIFT | PolyPhen | PROVEN | | rs no. | gnomAD | EXAC |
| C8ORF37 | c.55G>A | p.W185* | Hom | NA | NA | NA | Novel | rs748014296 | 2/246148 | 1/121412 |
| OFD1 | c.358A>G | p.T120A | Hem | 0.63 (tolerated) | 0.006 (benign) | −0.616 (netural) | Novel | rs755625951 | 4/178544 | 1/121388 |
| TULP1 | c.1255C>T | p.R419W | Hom | 0 (damaging) | 1 (probably damaging) | −7.976 (deleterious) | Novel | rs775334320 | 12/217192 | 6/121222 |
| RP1 | c.2285_2289delTAAAT | p.L762Yfs*17 | Het | NA | NA | NA | Novel | NA | NA | NA |

*Hom* homozygous, *Hem* hemizygous, *Het* heterozygous, *NA* not available

SIFT: http://sift.bii.a-star.edu.sg/; PolyPhen: http://genetics.bwh.harvard.edu/pph2/; PROVEN: http://provean.jcvi.org/index.php; gnomAD: http://gnomad.broadinstitute.org/; EXAC: http://exac.broadinstitute.org/

Chen *et al. J Transl Med* (2018) 16:145

Page 8 of 12

**Table 3 List of mutations reported in *C8ORF37*, *OFD1* and *TULP1* associated retinopathies**

| Gene | Variation | | | Disease | References |
|------|-----------|---|---|---------|------------|
| | Nucleotide | Amino acid | Domain | | |
| *C8ORF37* | c.155+2T>C | – | – | CRD | [56] |
| *C8ORF37* | c.156−2A>G | – | – | CRD | [15, 18] |
| *C8ORF37* | c.243+2T>C | – | – | RP | [21] |
| *C8ORF37* | c.244−2A>C | – | – | RP | [17] |
| *C8ORF37* | c.374+2T>C | – | – | EORD | [20] |
| *C8ORF37* | c.497>A | p.L166* | – | RP | [15, 18] |
| *C8ORF37* | c.529C>T | p.R177W | – | CRD, BBS | [15, 18, 19, 22] |
| *C8ORF37* | c.545A>G | p.Q182R | – | RP | [15, 18] |
| *C8ORF37* | c.555G>A | p.W185* | – | RP | [17], this study |
| *C8ORF37* | c.575delC | p.T192Mfs*28 | – | EORD | [20] |
| *OFD1* | | p.T120A | – | RP | This study |
| *OFD1* | IVS9+706A>G | p.N313fs*330 | Coiled coil domain | RP | [13] |
| *TULP1* | c.3G>A | p.M1I | – | RP | [25] |
| *TULP1* | c.99+1G>A | – | – | LCA, RP | [23, 26] |
| *TULP1* | c.280G>T | p.D94Y | – | LCA | [27] |
| *TULP1* | c.286_287delGA | p.E96Gfs*77 | – | RP | [57] |
| *TULP1* | c.350−2delAGA | – | – | RP | [28] |
| *TULP1* | c.394_417del | p.E120_D127del | – | RP | [29] |
| *TULP1* | c.539G>A | p.R180H | – | LCA | [30] |
| *TULP1* | c.627delC | p.S210Qfs*27 | – | LCA | [31] |
| *TULP1* | c.629C>G | p.S210* | – | RP | [32] |
| *TULP1* | c.718+2T>C | – | – | LCA, RP | [33] |
| *TULP1* | c.725_728delCCAA | p.P242Qfs*16 | – | LCA | [34] |
| *TULP1* | c.901C>T | p.Q301* | Tubby domain | LCA, CRD | [35, 36] |
| *TULP1* | c.937delC | p.Q301fs*9 | Tubby domain | RP | [28] |
| *TULP1* | c.932G>A | p.R311Q | Tubby domain | RP | [37] |
| *TULP1* | c.956G>A | p.G319D | Tubby domain | RP | [38] |
| *TULP1* | c.961T>G | p.Y321D | Tubby domain | LCA | [34] |
| *TULP1* | c.999+5G>C | – | Tubby domain | LCA, RP | [33] |
| *TULP1* | c.1025G>A | p.R342Q | Tubby domain | RP | [37] |
| *TULP1* | c.1047T>G | p.N349K | Tubby domain | RP | [39] |
| *TULP1* | c.1064A>T | p.D355V | Tubby domain | LCA | [34] |
| *TULP1* | c.1087G>A | p.G363R | Tubby domain | CRD | [40] |
| *TULP1* | c.1081C>T | p.R361* | Tubby domain | LCA | [41] |
| *TULP1* | c.1102G>T | p.G368W | Tubby domain | LCA | [26] |
| *TULP1* | c.1112+2T>C | – | Tubby domain | RP | [42] |
| *TULP1* | c.1113−2A>C | – | Tubby domain | LCA | [34] |
| *TULP1* | c.1138A>G | p.T380A | Tubby domain | LCA, RP | [43, 45, 46] |
| *TULP1* | c.1145T>C | p.F382S | Tubby domain | RP | [47] |
| *TULP1* | c.1198C>T | p.R400W | Tubby domain | LCA, RP, CRD | [26, 48, 49] |
| *TULP1* | c.1199G>A | p.A400Q | Tubby domain | RP | [50] |
| *TULP1* | c.1204G>T | p.E402* | Tubby domain | LCA | [26] |
| *TULP1* | c.1224+4A>G | – | Tubby domain | RP | [29] |
| *TULP1* | c.1246C>T | p.R416C | Tubby domain | RP | [25] |
| *TULP1* | c.1255C>T | p.R419W | Tubby domain | RP | This study |
| *TULP1* | c.1258C>A | p.R420S | Tubby domain | RCD | [51] |
| *TULP1* | c.1259G>C | p.R420P | Tubby domain | RP | [23] |
| *TULP1* | c.1318C>T | p.R440* | Tubby domain | LCA | [31] |

Chen *et al. J Transl Med (2018) 16:145*

Page 9 of 12

**Table 3 (continued)**

| Gene | Variation | | | Disease | References |
|------|-----------|--|--|---------|------------|
| | **Nucleotide** | **Amino acid** | **Domain** | | |
| *TULP1* | c.1349G>A | p.W450* | Tubby domain | LCA | [27] |
| *TULP1* | c.1376T>A | p.I459K | Tubby domain | RP | [23, 24] |
| *TULP1* | c.1376T>C | p.I459T | Tubby domain | RP | [42] |
| *TULP1* | c.1376_1377delTA | p.I459Rfs*12 | Tubby domain | LCA | [34] |
| *TULP1* | c.1381C>G | p.L461V | Tubby domain | LCA, RP | [33] |
| *TULP1* | c.1444C>T | p.R482W | Tubby domain | RP | [44, 48] |
| *TULP1* | c.1445G>A | p.A482Q | Tubby domain | RP | [46] |
| *TULP1* | c.1466A>G | p.K489R | Tubby domain | RP | [29, 43, 52, 57] |
| *TULP1* | c.1472T>C | p.F491L | Tubby domain | RP | [23] |
| *TULP1* | c.1495+1G>A | – | Tubby domain | RP | [24] |
| *TULP1* | c.1495+2_1495+3insT | – | Tubby domain | RP | [53] |
| *TULP1* | c.1495+4A>C | – | Tubby domain | RP | [57] |
| *TULP1* | c.1496−6C>A | – | Tubby domain | RP | [23, 29] |
| *TULP1* | c.1511_1521del | p.L504fs*140 | Tubby domain | RP | [44] |
| *TULP1* | c.1518C>A | p.F506L | Tubby domain | LCA | [31] |
| *TULP1* | c.1561C>T | p.P521S | Tubby domain | RP | [57] |
| *TULP1* | c.1582_1587dup | p.F528_A529dup | Tubby domain | LCA, RP | [54] |
| *TULP1* | c.1604T>C | p.F535S | Tubby domain | LCA | [55] |

*CRD* cone-rod dystrophy, *RP* retinitis pigmentosa, *EORD* early-onset retinal dystrophy, *BBS* Bardet–Biedl syndrome, *LCA* Leber congenital amaurosis

b), and were confirmed absent in 150 Chinese controls free of major ocular problems.

## Discussion

RP is a genetically heterogeneous disease with 83 disease causative genes and hundreds of mutations. In this report, molecular test reveals the coexistence of mutations affecting distinct RP causing genes in two RP families, thus providing novel insights into genetic assessments in complicated pedigrees. Among the four mutations identified in the two families, two were novel (*OFD1* p.T120A and *TULP1* p.R419W) and two were recurrent (*C8ORF37* p.W185* and *RP1* p.L762Yfs*17 [Human Gene Mutation Database ID: CD991855]).

*OFD1* mutations have been reported to cause X-linked recessive Joubert syndrome, orofaciodigital syndrome and isolated RP (Table 3) [12, 13]. OFD1, protein encoded by the *OFD1* gene, is a crucial component of the centrioles. OFD1 is involved in ciliogenesis regulation and exhibits neuroprotective roles [14]. Herein, a hemizygous *OFD1* missense mutation is associated with a severe form of RP presenting early onset age and fast disease progression. *C8ORF37* mutations correlate with a wide spectrum of autosomal recessive retinopathies ranging from RP to Bardet-Biedl syndrome (Table 3) [15–22]. The encoded C8ORF37 protein is a ciliary protein located at the base of the photoreceptor connecting cilia [16], while its role

in modulating retinal function is not fully elucidated. In this study, the patient carrying homozygous nonsense *C8ORF37* mutation presents early onset RP with macular involvement, which is similar to previous reports [15, 17]. *TULP1* mutations are implicated in autosomal recessive RP and LCA etiologies (Table 3) [22–57]. TULP1 protein plays crucial roles in maintaining retinal homeostasis. According to previous reports, TULP1 interacts and co-localizes with F-actin in photoreceptor cells of bovine retina [58], and RPE phagocytosis ability was remarkably reduced in *TULP1$^{-/-}$* mice [59]. Thus, TULP1 is required for maintaining regular functions of photoreceptors and RPE cells. We herein identified *TULP1* mutations in two siblings demonstrating RP with early onset and quick progression. Further confirmatory functional studies are still needed to better illustrated pathogenesis of the identified novel mutations.

## Conclusions

In summary, we demonstrate the coexistence of diverse inheritance modes and mutations affecting distinct disease causing genes in two RP families. Our findings reinforce the genetic complexity of RP, provide novel insights into the assessments of complicated pedigrees with consanguinity, and highlight the need for extensive molecular evaluations in such challenging families involving diverse inheritance modes and mutations.

Chen *et al. J Transl Med (2018) 16:145*

Page 10 of 12

## Additional files

**Additional file 1: Table S1.** Post-filtration variants in family A.

**Additional file 2: Table S2.** Post-filtration variants in family B.

**Additional file 3: Table S3.** Overview of data production.

**Additional file 4: Table S4.** Coverage for all exons in all known RP genes.

### Abbreviations
RP: retinitis pigmentosa; NGS: next-generation sequencing; WES: whole exome sequencing; bp: base pair; LM-PCR: ligation-mediated polymerase chain reaction; RPE: retinal pigment epithelium.

### Authors' contributions
XC, XS, YL, and ZL contributed equally to this report. All authors were involved in managing the patients. XC, BY and CZ wrote the report. XC, XS, YL and ZL did the genetic analysis and whole exome sequencing, and CZ reviewed the genetic results. All authors read and approved the final manuscript.

### Author details
<sup>1</sup> Department of Ophthalmology, State Key Laboratory of Reproductive Medicine, The First Affiliated Hospital of Nanjing Medical University, Nanjing, China. <sup>2</sup> Department of Ophthalmology and Vision Science, Eye & ENT Hospital, Shanghai Medical College, Fudan University, Shanghai, China. <sup>3</sup> Key Laboratory of Myopia of State Health Ministry (Fudan University) and Shanghai Key Laboratory of Visual Impairment and Restoration, Shanghai, China. <sup>4</sup> Department of Ophthalmology, Ningxia Eye Hospital, People Hospital of Ningxia Hui Autonomous Region (First Affiliated Hospital of Northwest University for Nationalities), Yinchuan, China. <sup>5</sup> Department of Ophthalmology, Children's Hospital of Zhengzhou, Zhengzhou, China.

### Competing interests
The authors declare that they have no competing interests.

### Availability of data and materials
The datasets used and/or analyzed during the current study are available from the corresponding author on reasonable request.

### Consent for publication
Yes.

### Ethics approval and consent to participate
Our study, conformed to the Declaration of Helsinki, was approved and prospectively reviewed by the local ethics committee of People Hospital of Ningxia Hui Autonomous Region. Written informed contents were obtained from all participants or their legal guardians before their enrollments.

## Publisher's Note
Springer Nature remains neutral with regard to jurisdictional claims in published maps and institutional affiliations.

### References
1. Anasagasti A, Irigoyen C, Barandika O, de Munain AL, Ruiz-Ederra J. Current mutation discovery approaches in retinitis pigmentosa. Vis Res. 2012;75:117–29.
2. Liu Y, Chen X, Xu Q, Gao X, Tam PO, Zhao K, Zhang X, Chen LJ, Jia W, Zhao Q, et al. SPP2 mutations cause autosomal dominant retinitis pigmentosa. Sci Rep. 2015;5:14867.
3. Hartong DT, Berson EL, Dryja TP. Retinitis pigmentosa. Lancet. 2006;368:1795–809.
4. Liu X, Xiao J, Huang H, Guan L, Zhao X, Xu Q, Zhang X, Pan X, Gu S, Chen Y, et al. Molecular genetic testing in clinical diagnostic assessments that demonstrate correlations in patients with autosomal recessive inherited retinal dystrophy. JAMA Ophthalmol. 2015;133:427–36.
5. Chen X, Sheng X, Liu X, Li H, Liu Y, Rong W, Ha S, Liu W, Kang X, Zhao K, Zhao C. Targeted next-generation sequencing reveals novel USH2A mutations associated with diverse disease phenotypes: implications for clinical and molecular diagnosis. PLoS ONE. 2014;9:e105439.
6. Sheng X, Chen X, Lei B, Chen R, Wang H, Zhang F, Rong W, Ha R, Liu Y, Zhao F, et al. Whole exome sequencing confirms the clinical diagnosis of Marfan syndrome combined with X-linked hypophosphatemia. J Transl Med. 2015;13:179.
7. Chen X, Sheng X, Zhuang W, Sun X, Liu G, Shi X, Huang G, Mei Y, Li Y, Pan X, et al. GUCA1A mutation causes maculopathy in a five-generation family with a wide spectrum of severity. Genet Med. 2017;19:945–54.
8. Challis D, Yu J, Evani US, Jackson AR, Paithankar S, Coarfa C, Milosavljevic A, Gibbs RA, Yu F. An integrative variant analysis suite for whole exome next-generation sequencing data. BMC Bioinform. 2012;13:8.
9. Zhao C, Lu S, Zhou X, Zhang X, Zhao K, Larsson C. A novel locus (RP33) for autosomal dominant retinitis pigmentosa mapping to chromosomal region 2cen-q12.1. Hum Genet. 2006;119:617–23.
10. Arnold K, Bordoli L, Kopp J, Schwede T. The SWISS-MODEL workspace: a web-based environment for protein structure homology modelling. Bioinformatics. 2006;22:195–201.
11. McDowall J, Hunter S. InterPro protein classification. Methods Mol Biol. 2011;694:37–47.
12. Coene KL, Roepman R, Doherty D, Afroze B, Kroes HY, Letteboer SJ, Ngu LH, Budny B, van Wijk E, Gorden NT, et al. OFD1 is mutated in X-linked Joubert syndrome and interacts with LCA5-encoded lebercilin. Am J Hum Genet. 2009;85:465–81.
13. Webb TR, Parfitt DA, Gardner JC, Martinez A, Bevilacqua D, Davidson AE, Zito I, Thiselton DL, Ressa JH, Apergi M, et al. Deep intronic mutation in OFD1, identified by targeted genomic next-generation sequencing, causes a severe form of X-linked retinitis pigmentosa (RP23). Hum Mol Genet. 2012;21:3647–54.
14. Wang J, Chen X, Wang F, Zhang J, Li P, Li Z, Xu J, Gao F, Jin C, Tian H, et al. OFD1, as a ciliary protein, exhibits neuroprotective function in photoreceptor degeneration models. PLoS ONE. 2016;11:e0155860.
15. Estrada-Cuzcano A, Neveling K, Kohl S, Banin E, Rotenstreich Y, Sharon D, Falik-Zaccai TC, Hipp S, Roepman R, Wissinger B, et al. Mutations in C8orf37, encoding a ciliary protein, are associated with autosomal-recessive retinal dystrophies with early macular involvement. Am J Hum Genet. 2012;90:102–9.
16. Heon E, Kim G, Qin S, Garrison JE, Tavares E, Vincent A, Nuangchamnong N, Scott CA, Slusarski DC, Sheffield VC. Mutations in C8ORF37 cause Bardet Biedl syndrome (BBS21). Hum Mol Genet. 2016;25:2283–94.
17. Ravesh Z, El Asrag ME, Weisschuh N, McKibbin M, Reuter P, Watson CM, Baumann B, Poulter JA, Sajid S, Panagiotou ES, et al. Novel C8orf37 mutations cause retinitis pigmentosa in consanguineous families of Pakistani origin. Mol Vis. 2015;21:236–43.
18. van Huet RA, Estrada-Cuzcano A, Banin E, Rotenstreich Y, Hipp S, Kohl S, Hoyng CB, den Hollander AI, Collin RW, Klevering BJ. Clinical characteristics of rod and cone photoreceptor dystrophies in patients with mutations in the C8orf37 gene. Invest Ophthalmol Vis Sci. 2013;54:4683–90.

Chen *et al. J Transl Med* (2018) 16:145

Page 11 of 12

19. Khan AO, Decker E, Bachmann N, Bolz HJ, Bergmann C. C8orf37 is mutated in Bardet-Biedl syndrome and constitutes a locus allelic to non-syndromic retinal dystrophies. Ophthalmic Genet. 2016;37:290–3.

20. Katagiri S, Hayashi T, Yoshitake K, Akahori M, Ikeo K, Gekka T, Tsuneoka H, Iwata T. Novel C8orf37 mutations in patients with early-onset retinal dystrophy, macular atrophy, cataracts, and high myopia. Ophthalmic Genet. 2016;37:68–75.

21. Jinda W, Taylor TD, Suzuki Y, Thongnoppakhun W, Limwongse C, Lertrit P, Suriyaphol P, Trinavarat A, Atchaneeyasakul LO. Whole exome sequencing in Thai patients with retinitis pigmentosa reveals novel mutations in six genes. Invest Ophthalmol Vis Sci. 2014;55:2259–68.

22. Lazar CH, Mutsuddi M, Kimchi A, Zelinger L, Mizrahi-Meissonnier L, Marks-Ohana D, Boleda A, Ratnapriya R, Sharon D, Swaroop A, Banin E. Whole exome sequencing reveals GUCY2D as a major gene associated with cone and cone-rod dystrophy in Israel. Invest Ophthalmol Vis Sci. 2014;56:420–30.

23. Hagstrom SA, North MA, Nishina PL, Berson EL, Dryja TP. Recessive mutations in the gene encoding the tubby-like protein TULP1 in patients with retinitis pigmentosa. Nat Genet. 1998;18:174–6.

24. Banerjee P, Kleyn PW, Knowles JA, Lewis CA, Ross BM, Parano E, Kovats SG, Lee JJ, Penchaszadeh GK, Ott J, et al. TULP1 mutation in two extended Dominican kindreds with autosomal recessive retinitis pigmentosa. Nat Genet. 1998;18:177–9.

25. Katagiri S, Akahori M, Sergeev Y, Yoshitake K, Ikeo K, Furuno M, Hayashi T, Kondo M, Ueno S, Tsunoda K, et al. Whole exome analysis identifies frequent CNGA1 mutations in Japanese population with autosomal recessive retinitis pigmentosa. PLoS ONE. 2014;9:e108721.

26. Hanein S, Perrault I, Gerber S, Tanguy G, Barbet F, Ducroq D, Calvas P, Dollfus H, Hamel C, Lopponen T, et al. Leber congenital amaurosis: comprehensive survey of the genetic heterogeneity, refinement of the clinical definition, and genotype-phenotype correlations as a strategy for molecular diagnosis. Hum Mutat. 2004;23:306–17.

27. Beryozkin A, Zelinger L, Bandah-Rozenfeld D, Shevach E, Harel A, Storm T, Sagi M, Eli D, Merin S, Banin E, Sharon D. Identification of mutations causing inherited retinal degenerations in the israeli and palestinian populations using homozygosity mapping. Invest Ophthalmol Vis Sci. 2014;55:1149–60.

28. Paloma E, Hjelmqvist L, Bayes M, Garcia-Sandoval B, Ayuso C, Balcells S, Gonzalez-Duarte R. Novel mutations in the TULP1 gene causing autosomal recessive retinitis pigmentosa. Invest Ophthalmol Vis Sci. 2000;41:656–9.

29. Gu S, Lennon A, Li Y, Lorenz B, Fossarello M, North M, Gal A, Wright A. Tubby-like protein-1 mutations in autosomal recessive retinitis pigmentosa. Lancet. 1998;351:1103–4.

30. Gonzalez-del Pozo M, Borrego S, Barragan I, Pieras JI, Santoyo J, Matamala N, Naranjo B, Dopazo J, Antinolo G. Mutation screening of multiple genes in Spanish patients with autosomal recessive retinitis pigmentosa by targeted resequencing. PLoS ONE. 2011;6:e27894.

31. Wang H, Wang X, Zou X, Xu S, Li H, Soens ZT, Wang K, Li Y, Dong F, Chen R, Sui R. Comprehensive molecular diagnosis of a large Chinese Leber congenital amaurosis cohort. Invest Ophthalmol Vis Sci. 2015;56:3642–55.

32. Glockle N, Kohl S, Mohr J, Scheurenbrand T, Sprecher A, Weisschuh N, Bernd A, Rudolph G, Schubach M, Poloschek C, et al. Panel-based next generation sequencing as a reliable and efficient technique to detect mutations in unselected patients with retinal dystrophies. Eur J Hum Genet. 2014;22:99–104.

33. den Hollander AI, Lopez I, Yzer S, Zonneveld MN, Janssen IM, Strom TM, Hehir-Kwa JY, Veltman JA, Arends ML, Meitinger T, et al. Identification of novel mutations in patients with Leber congenital amaurosis and juvenile RP by genome-wide homozygosity mapping with SNP microarrays. Invest Ophthalmol Vis Sci. 2007;48:5690–8.

34. Wang X, Wang H, Sun V, Tuan HF, Keser V, Wang K, Ren H, Lopez I, Zaneveld JE, Siddiqui S, et al. Comprehensive molecular diagnosis of 179 Leber congenital amaurosis and juvenile retinitis pigmentosa patients by targeted next generation sequencing. J Med Genet. 2013;50:674–88.

35. Li Y, Wang H, Peng J, Gibbs RA, Lewis RA, Lupski JR, Mardon G, Chen R. Mutation survey of known LCA genes and loci in the Saudi Arabian population. Invest Ophthalmol Vis Sci. 2009;50:1336–43.

36. Khan AO, Bergmann C, Eisenberger T, Bolz HJ. A TULP1 founder mutation, p.Gln301*, underlies a recognisable congenital rod-cone dystrophy phenotype on the Arabian Peninsula. Br J Ophthalmol. 2015;99:488–92.

37. Hebrard M, Manes G, Bocquet B, Meunier I, Coustes-Chazalette D, Herald E, Senechal A, Bolland-Auge A, Zelenika D, Hamel CP. Combining gene mapping and phenotype assessment for fast mutation finding in non-consanguineous autosomal recessive retinitis pigmentosa families. Eur J Hum Genet. 2011;19:1256–63.

38. Consugar MB, Navarro-Gomez D, Place EM, Bujakowska KM, Sousa ME, Fonseca-Kelly ZD, Taub DG, Janessian M, Wang DY, Au ED, et al. Panel-based genetic diagnostic testing for inherited eye diseases is highly accurate and reproducible, and more sensitive for variant detection, than exome sequencing. Genet Med. 2015;17:253–61.

39. Kannabiran C, Singh H, Sahini N, Jalali S, Mohan G. Mutations in TULP1, NR2E3, and MFRP genes in Indian families with autosomal recessive retinitis pigmentosa. Mol Vis. 2012;18:1165–74.

40. Boulanger-Scemama E, El Shamieh S, Demontant V, Condroyer C, Antonio A, Michiels C, Boyard F, Saraiva JP, Letexier M, Souied E, et al. Next-generation sequencing applied to a large French cone and cone-rod dystrophy cohort: mutation spectrum and new genotype-phenotype correlation. Orphanet J Rare Dis. 2015;10:85.

41. Guo Y, Prokudin I, Yu C, Liang J, Xie Y, Flaherty M, Tian L, Crofts S, Wang F, Snyder J, et al. Advantage of whole exome sequencing over allele-specific and targeted segment sequencing in detection of novel TULP1 mutation in Leber congenital amaurosis. Ophthalmic Genet. 2015;36:333–8.

42. Wang F, Wang H, Tuan HF, Nguyen DH, Sun V, Keser V, Bowne SJ, Sullivan LS, Luo H, Zhao L, et al. Next generation sequencing-based molecular diagnosis of retinitis pigmentosa: identification of a novel genotype-phenotype correlation and clinical refinements. Hum Genet. 2014;133:331–45.

43. Iqbal M, Naeem MA, Riazuddin SA, Ali S, Farooq T, Qazi ZA, Khan SN, Husnain T, Riazuddin S, Sieving PA, Hejtmancik JF. Association of pathogenic mutations in TULP1 with retinitis pigmentosa in consanguineous Pakistani families. Arch Ophthalmol. 2011;129:1351–7.

44. den Hollander AI, van Lith-Verhoeven JJ, Arends ML, Strom TM, Cremers FP, Hoyng CB. Novel compound heterozygous TULP1 mutations in a family with severe early-onset retinitis pigmentosa. Arch Ophthalmol. 2007;125:932–5.

45. McKibbin M, Ali M, Mohamed MD, Booth AP, Bishop F, Pal B, Springell K, Raashid Y, Jafri H, Inglehearn CF. Genotype-phenotype correlation for leber congenital amaurosis in Northern Pakistan. Arch Ophthalmol. 2010;128:107–13.

46. Ajmal M, Khan MI, Micheal S, Ahmed W, Shah A, Venselaar H, Bokhari H, Azam A, Waheed NK, Collin RW, et al. Identification of recurrent and novel mutations in TULP1 in Pakistani families with early-onset retinitis pigmentosa. Mol Vis. 2012;18:1226–37.

47. Kondo H, Qin M, Mizota A, Kondo M, Hayashi H, Hayashi K, Oshima K, Tahira T. A homozygosity-based search for mutations in patients with autosomal recessive retinitis pigmentosa, using microsatellite markers. Invest Ophthalmol Vis Sci. 2004;45:4433–9.

48. Chen Y, Zhang Q, Shen T, Xiao X, Li S, Guan L, Zhang J, Zhu Z, Yin Y, Wang P, et al. Comprehensive mutation analysis by whole-exome sequencing in 41 Chinese families with Leber congenital amaurosis. Invest Ophthalmol Vis Sci. 2013;54:4351–7.

49. Jacobson SG, Cideciyan AV, Huang WC, Sumaroka A, Roman AJ, Schwartz SB, Luo X, Sheplock R, Dauber JM, Swider M, Stone EM. TULP1 mutations causing early-onset retinal degeneration: preserved but insensitive macular cones. Invest Ophthalmol Vis Sci. 2014;55:5354–64.

50. Singh HP, Jalali S, Narayanan R, Kannabiran C. Genetic analysis of Indian families with autosomal recessive retinitis pigmentosa by homozygosity screening. Invest Ophthalmol Vis Sci. 2009;50:4065–71.

51. Roosing S, van den Born LI, Hoyng CB, Thiadens AA, de Baere E, Collin RW, Koenekoop RK, Leroy BP, van Moll-Ramirez N, Venselaar H, et al. Maternal uniparental isodisomy of chromosome 6 reveals a TULP1 mutation as a novel cause of cone dysfunction. Ophthalmology. 2013;120:1239–46.

52. Maria M, Ajmal M, Azam M, Waheed NK, Siddiqui SN, Mustafa B, Ayub H, Ali L, Ahmad S, Micheal S, et al. Homozygosity mapping and targeted sanger sequencing reveal genetic defects underlying inherited retinal disease in families from pakistan. PLoS ONE. 2015;10:e0119806.

53. Abbasi AH, Garzozi HJ, Ben-Yosef T. A novel splice-site mutation of TULP1 underlies severe early-onset retinitis pigmentosa in a consanguineous Israeli Muslim Arab family. Mol Vis. 2008;14:675–82.

Chen *et al. J Transl Med* (2018) 16:145

Page 12 of 12

54. Mataftsi A, Schorderet DF, Chachoua L, Boussalah M, Nouri MT, Bar-thelmes D, Borruat FX, Munier FL. Novel TULP1 mutation causing Leber congenital amaurosis or early onset retinal degeneration. Invest Ophthalmol Vis Sci. 2007;48:5160–7.

55. Eisenberger T, Neuhaus C, Khan AO, Decker C, Preising MN, Friedburg C, Bieg A, Gliem M, Charbel Issa P, Holz FG, et al. Increasing the yield in targeted next-generation sequencing by implicating CNV analysis, non-coding exons and the overall variant load: the example of retinal dystrophies. PLoS ONE. 2013;8:e78496.

56. Rahner N, Nuernberg G, Finis D, Nuernberg P, Royer-Pokora B. A novel C8orf37 splice mutation and genotype-phenotype correlation for cone-rod dystrophy. Ophthalmic Genet. 2016;37:294–300.

57. Ullah I, Kabir F, Iqbal M, Gottsch CB, Naeem MA, Assir MZ, Khan SN, Akram J, Riazuddin S, Ayyagari R, et al. Pathogenic mutations in TULP1 responsible for retinitis pigmentosa identified in consanguineous familial cases. Mol Vis. 2016;22:797–815.

58. Xi Q, Pauer GJ, Marmorstein AD, Crabb JW, Hagstrom SA. Tubby-like protein 1 (TULP1) interacts with F-actin in photoreceptor cells. Invest Ophthalmol Vis Sci. 2005;46:4754–61.

59. Caberoy NB, Maiguel D, Kim Y, Li W. Identification of tubby and tubby-like protein 1 as eat-me signals by phage display. Exp Cell Res. 2010;316:245–57.